

## Transient analysis of frictionally excited thermoelastic instability in multi-disk clutches and brakes

L. Afferrante<sup>a,b</sup>, M. Ciavarella<sup>b,c</sup>, P. Decuzzi<sup>a,b,\*</sup>, G. Demelio<sup>a,b</sup>

<sup>a</sup> Dipartimento di Ingegneria Meccanica e Gestionale (DIMEG), Politecnico di Bari-Viale Japigia, 182-70126 Bari, Italy

<sup>b</sup> Center of Excellence in Computational Mechanics (CEMeC) Politecnico di Bari-Viale Japigia, 182-70126 Bari, Italy

<sup>c</sup> CNR-IRIS Computational Mechanics of Solids, Street Crocefisso, 2/B-70126 Bari, Italy

Received 23 April 2002; accepted 29 October 2002

### Abstract

A 2D multilayered model has been considered to estimate the transient evolution of temperature and pressure perturbations in multi-disk clutches and brakes during operation. The model proposed by Decuzzi et al. [1] has been modified here to estimate the variation of  $b$ —perturbation growth rate—with  $V$ —relative sliding speed. It has been verified that the perturbation with the lowest critical speed has also the highest growth rate, and that low frequency perturbations are less critical than high frequency perturbations, at fixed critical speed. Therefore, when comparing perturbations with identical critical speed, those with higher wave numbers are responsible for more intense thermomechanical damages. Also, for perturbations with wave number smaller than the critical  $m_{cr}$ , the temperature increases with  $m$ ; vice versa for perturbations with wave number larger than  $m_{cr}$  the temperature decreases with  $m$ . A reduction in thickness ratio  $a_1/a_2$  between friction and metal disks has the effect of increasing the temperature and growth rate. An approximate formula for the temperature variation with time has been derived for a linearly decreasing engagement speed.

© 2002 Elsevier Science B.V. All rights reserved.

**Keywords:** Brakes and clutches; Hot spotting; Thermoelastic instability

### 1. Introduction

It is well known since the pioneering experiments of Parker and Marshall [2] that concentration of frictional heating over zones smaller than the nominal frictional interface can occur in clutches and brakes, thus leading to large localized temperature and mechanical pressure. In 1969, Barber [3] has proposed a physical explanation of the phenomenon introducing the idea of frictionally excited thermoelastic instability (TEI): non-uniform thermomechanical deformations modify the surface profile and contact pressure which in turn alters the frictionally heat generated at the sliding interface, thus modifying again the thermomechanical deformations. Few years later, in 1973, Burton et al. [4] presented the first theoretical model of TEI and introduced the idea of a critical speed  $V_{cr}$  above which the system is always thermoelastically unstable. Since then, several experimental and theoretical analysis have been carried out aiming at better understanding the phenomenon and defining the governing parameters. Most of the theoretical works have been focused on the analysis of the onset of instability

and were dedicated to the estimation of the critical speed  $V_{cr}$  for different geometries and material properties (see Lee and Barber [5,6]; Yi et al. [7], Decuzzi et al. [1]; Decuzzi and Demelio [8], Davis et al. [9]).

Nowadays the rush towards higher performances has increased sliding operative speeds of clutches and brakes. Also, in practical applications engagement speeds might be larger than critical speeds for TEI, and typical service consists in frequent and quick engagements cycles, so that clutches and brakes operates predominantly in a transient regime. Consequently, it has been recognized the importance of studying the occurrence and evolution of TEI for a time-dependent sliding speed. One of the first transient analysis of a multi-disk clutch was performed by Zagrodzki [10] who, to make the problem numerically tractable, combined a finite difference discretization in time for solving the thermal problem with a finite element scheme for solving the elasticity contact problem. He monitored the evolution with time of the temperature distribution and mechanical deformations at the disks' surface and along the pack of disks. A finite difference discretization was also used by Jang and Khonsari [11] in modelling the transient thermohydrodynamic engagement of a single-disk wet clutch. More recently, efficient transient analysis of clutch/brake

\* Corresponding author. Tel.: +39-80-596-2718; fax: +39-80-596-2777.  
E-mail address: [p.decuzzi@poliba.it](mailto:p.decuzzi@poliba.it) (P. Decuzzi).

**Nomenclature**

$a_i$	half thickness of layer $i$ (m)
$b$	growth rate ( $s^{-1}$ )
$c$	perturbation absolute speed (m/s)
$c_i$	perturbation relative speed with respect to layer $i$ (m/s)
$c_{pi}$	specific heat of layer $i$ (J/kg °C)
$E_i$	Young's modulus of layer $i$ (N/m <sup>2</sup> )
$f$	frictional coefficient
$j$	imaginary unit
$k_i$	diffusivity of layer $i$ (m <sup>2</sup> /s)
$K_i$	thermal conductivity of layer $i$ (W/m °C)
$m$	wave number (m <sup>-1</sup> )
$m_{cr}$	critical wave number (m <sup>-1</sup> )
$N$	hot spots number
$p$	contact pressure distribution (N/m <sup>2</sup> )
$q$	heat flux per unit area (W/m <sup>2</sup> )
$q_{yi}$	heat flux per unit area entering layer $i$ (W/m <sup>2</sup> )
$t_0$	stopping time (s)
$t$	time (s)
$T_0$	initial amplitude of the perturbed temperature field (°C)
$T_i$	temperature field in the layer $i$ (°C)
$u_i$	displacements at the sliding interface of layer $i$ (m)
$V_0$	initial sliding speed (m/s)
$V$	sliding speed (m/s)
$V_{cr}$	critical sliding speed (m/s)

**Greek letters**

$\alpha_i$	thermal expansion coefficient in layer $i$ (°C <sup>-1</sup> )
$\lambda$	wave length of the perturbation (m)
$\mu_i$	shear modulus in layer $i$ (N/m <sup>2</sup> )
$\nu_i$	Poisson's coefficient in layer $i$
$\sigma_{yy_i}$	normal tractions at the sliding interface of layer $i$ (N/m <sup>2</sup> )
$\sigma_{xy_i}$	shear tractions at the sliding interface of layer $i$ (N/m <sup>2</sup> )
$\rho_i$	density of layer $i$ (Kg/m <sup>3</sup> )
$\phi_i, \omega_i$	Green and Zerna harmonic potential functions
$\psi_i$	thermoelastic strain potential

engagement have been proposed by Al-Shabibi and Barber [12] adopting a reduced order model.

In this work, a 2D multi-disk model is used, derived by Decuzzi et al. [1], which is based on a small perturbation analysis: it is assumed that the otherwise uniform contact pressure at the sliding interface is perturbed. It is then estimated: (i) the variation of the growth rate  $b$  of the perturbed solution with the sliding operating speed  $V > V_{cr}$ ; (ii) the effect of the wave number and disk thickness on the  $b(V)$  relation; (iii) the evolution with time of the surface temperature and pressure distribution, assuming a linear variation

of the sliding speed in the engagement process; (iv) an approximate formula for the temperature variation with time.

**2. Model and formulation**

Multi-disk brakes and clutches are made up of homogeneous metal disks and friction disks, where a core metal layer is covered on both sides by friction linings. In the present formulation, a multilayered structure is employed to reproduce a multi-disk clutch or brake as proposed in Decuzzi et al. [1]. The system is symmetrical with respect to middle-planes of the friction and metal layers, thus the analysis of the problem can be condensed to a half frictional layer (1) sliding on half metal layer (2) (Fig. 1), where suitable boundary conditions are imposed at the planes of symmetry. Inspired by Burton et al. analysis [4], the thermoelastic stability of the system is assessed by perturbing the otherwise uniform contact pressure at the sliding interface, that is to say

$$p(x, t) = p_0 e^{bt} e^{jmx} \quad (1)$$

where the growth rate  $b$  could take up negative values ( $b < 0$ ) for stable perturbation, positive values ( $b > 0$ ) for unstable perturbation, and zero ( $b = 0$ ) at the onset of instability, for which the critical sliding speed  $V_{cr}$  can be determined. In Fig. 1 two frames of reference ( $x_1, y_1$ ) and ( $x_2, y_2$ ) are fixed on the middle-planes of the two layers, while a third frame ( $x, y$ ) is moving with the perturbation having absolute speed  $c$ . The migration speed  $c_i$  is defined as the relative speed of the perturbation with respect to layer  $i$ , i.e.  $c_i = c - V_i$ .

The following formulation is an extension of that presented in Decuzzi et al. [1], where a non-zero growth rate,  $b$  is considered. Therefore, only the main features of the method are presented in the sequel. The reader is then referred to the above paper for a more detailed and comprehensive description of the possible sets of boundary conditions and physical meaning for the migration speed  $c_i$ .

**2.1. Temperature field**

The temperature distribution is governed by Fourier's equation  $k_i \nabla^2 T_i = \partial T_i / \partial t$ , where  $k_i = K_i / \rho_i c_{pi}$  is thermal

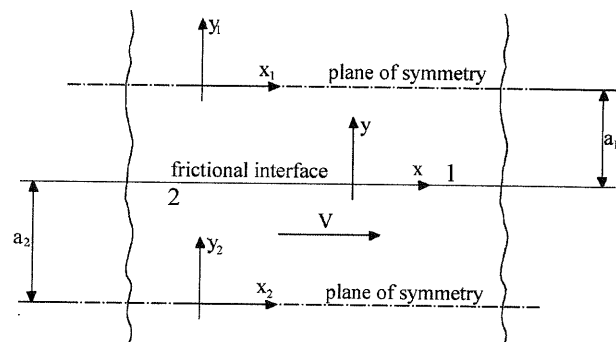


Fig. 1. Metal half layer (2) in sliding contact with friction half layer (1) with relative speed  $V$ .

diffusivity,  $K_i$  the thermal conductivity,  $\rho_i$  the density and  $c_{pi}$  the specific heat of the material  $i$ . The perturbed solution of the above equation is given as

$$T_i(x_i, y_i, t) = (A_i e^{\lambda_i y_i} + B_i e^{-\lambda_i y_i}) e^{bt} e^{jm(x_i - c_i t)} \quad (2)$$

with

$$\lambda_i(m, b, c_i) = \sqrt{\left(m^2 + \frac{b}{k_i}\right) - j \left(\frac{mc_i}{k_i}\right)} \quad (3)$$

where the four constants  $A_i$  and  $B_i$  ( $i = 1, 2$ ) are defined by the thermal boundary conditions:

- continuity of the temperature field at the sliding interface ( $y = 0$ ):

$$T_1(x, y; t)_{y=0} = T_0 e^{bt} e^{jmx} = T_0 e^{bt} e^{jmx} = T_2(x, y; t)_{y=0} \quad (4)$$

being from (2),

$$T_0 = A_1 + B_1 = A_2 + B_2 \quad (5)$$

- for symmetrical layers, the heat flux through the middle-plane ( $y_i = 0$ ) is zero:  $q_{yi}|_{y_i=0} = -K_i (\partial T_i / \partial y)|_{y_i=0} = 0$ ;
- for antisymmetrical layers, the temperature at the middle-plane ( $y_i = 0$ ) is zero:  $T_i|_{y_i=0} = 0$ ;

Therefore, after simple algebraic manipulation, it is found

$$T_i(x_i, y_i, t) = T_0 \frac{g[(-1)^i \lambda_i y_i]}{g[\lambda_i a_i]} e^{bt+jmx} \quad (6)$$

where  $g(\cdot) = \cosh(\cdot)$  for symmetrical layers and  $g(\cdot) = \sinh(\cdot)$  for antisymmetrical layers.

## 2.2. Thermoelastic stress and strain fields

The general solution of the thermoelastic problem is attained by superimposing a particular solution on the general isothermal elasticity problem.

As suggested by Barber ([13], Section 12), the particular solution of the thermoelastic problem may be expressed in terms of the strain potential  $\psi$ , satisfying the equation  $\nabla^2 \psi_i = \beta_i T_i$ ,

$$\psi_i = \frac{\beta_i T_0}{\lambda_i^2 - m^2} \left[ \frac{g(\lambda_i y_i)}{g(\lambda_i a_i)} - \frac{g(my_i)}{g(ma_i)} \right] e^{bt+jmx} \quad \text{with} \quad (7)$$

$$\beta_i = 2\mu_i \alpha_i \frac{1 + \nu_i}{1 - \nu_i}$$

where  $\alpha_i$  is the coefficient of thermal expansion,  $\mu_i = E_i / [2(1 + \nu_i)]$  is the shear modulus and  $E_i, \nu_i$  the Young and Poisson moduli, respectively. The displacement and stress fields are given by:

$$u_{xi} = \frac{1}{2\mu_i} \frac{\partial \psi_i}{\partial x}; \quad u_{yi} = \frac{1}{2\mu_i} \frac{\partial \psi_i}{\partial y}; \quad \sigma_{yyi} = -\frac{\partial^2 \psi_i}{\partial x^2};$$

$$\sigma_{xyi} = \frac{\partial^2 \psi_i}{\partial x \partial y} \quad (8)$$

Whilst, the general solution is obtained by employing the Green and Zerna ([14], Sections 12 and 13.2) harmonic potential functions  $\phi_i$  and  $\omega_i$  given by:

$$\phi_i = C_i \frac{g(my_i)}{g(ma_i)} e^{jmx}; \quad \omega_i = D_i \frac{g'(my_i)}{g'(ma_i)} e^{jmx} \quad (9)$$

with the displacement and stress fields

$$u_{xi} = \frac{1}{2\mu_i} \frac{\partial \phi_i}{\partial x} + \frac{1}{2\mu_i} y_i \frac{\partial \omega_i}{\partial x};$$

$$u_{yi} = \frac{1}{2\mu_i} \frac{\partial \phi_i}{\partial y} + \frac{1}{2\mu_i} y_i \frac{\partial \omega_i}{\partial y} - \frac{3 - 4\nu_i}{2\mu_i} \omega_i;$$

$$\sigma_{xxi} = \frac{\partial^2 \phi_i}{\partial x^2} + y_i \frac{\partial^2 \omega_i}{\partial x^2} - 2\nu_i \frac{\partial \omega_i}{\partial y};$$

$$\sigma_{yyi} = -\frac{\partial^2 \phi_i}{\partial y^2} + y_i \frac{\partial^2 \omega_i}{\partial y^2} - 2(1 - \nu_i) \frac{\partial \omega_i}{\partial y};$$

$$\sigma_{xyi} = \frac{\partial^2 \phi_i}{\partial x \partial y} + y_i \frac{\partial^2 \omega_i}{\partial x \partial y} - (1 - 2\nu_i) \frac{\partial \omega_i}{\partial x} \quad (10)$$

where the apex denotes differentiation and  $g(\cdot)$  is defined as above. Notice that for symmetrical layers  $u_{yi} = 0$  and  $\sigma_{xyi} = 0$  at  $y_i = 0$ , whilst for antisymmetrical layers  $u_{xi} = 0$  and  $\sigma_{yyi} = 0$  at  $y_i = 0$ . The four constants  $C_i$  and  $D_i$  ( $i = 1, 2$ ) can be calculated by imposing the mechanical conditions at the frictional surface ( $y = 0$ ), that is to say

$$u_{y1} - u_{y2} = 0; \quad \sigma_{yy1} - \sigma_{yy2} = 0 \quad (11)$$

$$\sigma_{xy1} - \sigma_{xy2} = 0; \quad \sigma_{xy1} + f\sigma_{yy1} = 0 \quad (12)$$

The pressure amplitude  $p_0$  at frictional interface is

$$p(x, t) = p_0 e^{bt} e^{jmx} = -\sigma_{yy1} \quad (13)$$

## 2.3. Characteristic equation

The fourth thermal boundary condition imposes energy conservation at the sliding interface, that is to say the frictional heat flux  $q = fVp$  must equal the heat partitioning between the two layers,

$$q_{y1} - q_{y2} = -K_1 \frac{\partial T_1}{\partial y} \Big|_{y=0} + K_2 \frac{\partial T_2}{\partial y} \Big|_{y=0} = fVp \quad (14)$$

From (1), (6) and (14) the following not linear complex characteristic equation is derived

$$\left[ K_1 \lambda_1 \frac{g'_1(\lambda_1 a_1)}{g_1(\lambda_1 a_1)} + K_2 \lambda_2 \frac{g'_2(\lambda_2 a_2)}{g_2(\lambda_2 a_2)} \right] T_0 - fVp_0 = 0 \quad (15)$$

For fixed material properties and geometry ( $m$  and  $a_1/a_2$ ), the real  $f_{Re}$  and imaginary  $f_{Im}$  parts of (Eq. (15)) together with the kinematics condition  $V = c_1 - c_2$  provide a non-linear system of three equations in the four unknowns  $V, b, c_1$  and  $c_2$ . Hence, by fixing  $b = 0$ , the critical speed  $V_{cr}$  is determined as from Decuzzi et al. [1], conversely by fixing the sliding speed  $V$ , the variation of the growth rate  $b$  with  $V$  is estimated. The above system of complex equations is solved by a classical bisection method.

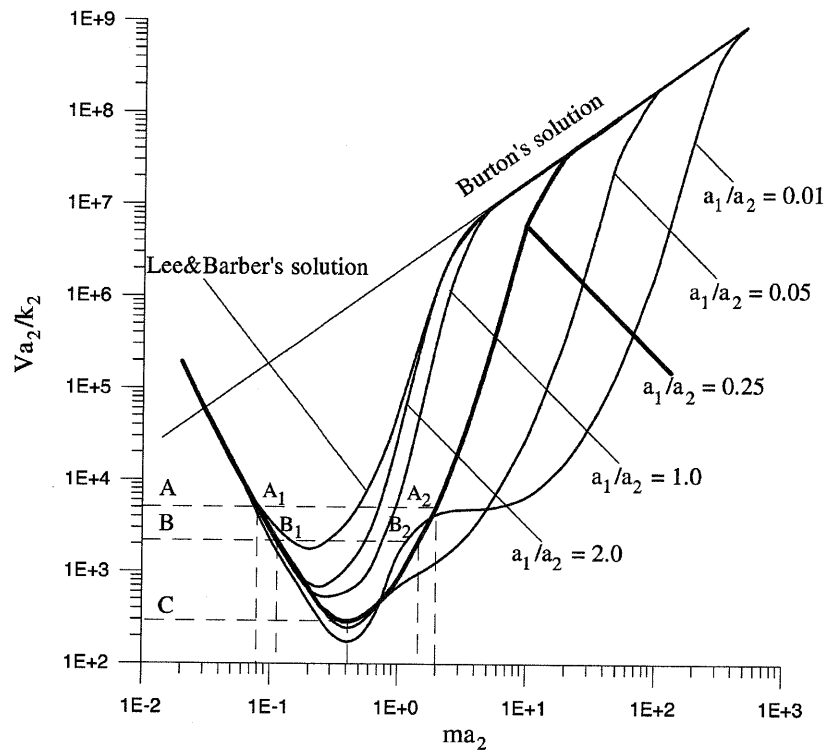


Fig. 2. Variation of the dimensionless critical speed  $Va_2/k_2$  against the wave parameter  $ma_2$  for different values of the thickness ratio  $a_1/a_2$ .

### 3. Results

The geometrical symmetry of the system leads to two possible sets of boundary conditions to be prescribed at the layers' mid plane: antisymmetric or symmetric. As shown in Decuzzi et al. [1], the most critical condition is for the antisymmetric case on the metal layer and symmetric case on the friction layer. Therefore, the results in the sequel are for the asymmetric/symmetric case, i.e. the most critical condition.

The well-known behavior of the dimensionless critical speed  $V_{cr}(=V_{cr}a_2/k_2)$  against the wave number  $ma_2$  for different values of the thickness ratio  $a_1/a_2$  is plotted in Fig. 2.

- the critical sliding speed reduces as the thickness ratio decreases;
- the Burton's solution is approached for  $ma_2 \rightarrow \infty$ ;
- the Lee and Barber solution is approached for  $a_1/a_2 \rightarrow \infty$ .

The material properties used throughout the paper are those listed in Table 1, typical of automotive applications. Three different representative values of the sliding speed for  $a_1/a_2 = 0.25$  have been highlighted with the letters A, B and C. For  $a_2 = 3$  (mm), two different perturbation wave numbers  $m_{A_1} = 26.53$  ( $m^{-1}$ ) and  $m_{A_2} = 666.67$  ( $m^{-1}$ );  $m_{B_1} = 38.15$  ( $m^{-1}$ ) and  $m_{B_2} = 500$  ( $m^{-1}$ ), correspond at A and B, respectively. Whilst C is the most critical condition with  $m_{cr} = m_C = 136.67$  ( $m^{-1}$ ).

#### 3.1. The growth rate $b$

In this section, the estimation of the growth rate for sliding speeds larger than the critical value has been presented. By doing so, the following two questions can be answered: how fast the perturbation grows beyond the onset of instability and how fast the system is thermally and mechanically damaged by hot spots formation. Also, in order to estimate the variation of the temperature distribution during engagement, it is necessary to know the growth rate  $b$  at

Table 1  
Material properties for metal (cast iron) and friction layers

Material	$E$ ( $N/m^2 \times 10^9$ )	$\nu$	$\alpha$ ( $^{\circ}C^{-1} \times 10^{-6}$ )	$K$ ( $W/m^{\circ}C$ )	$k$ ( $m^2/sec \times 10^{-6}$ )
Cast iron	125	0.25	12	54	12.98
Brake friction material	0.53	0.25	30	0.5	0.269
Clutch friction material	0.3	0.12	14	0.241	0.13

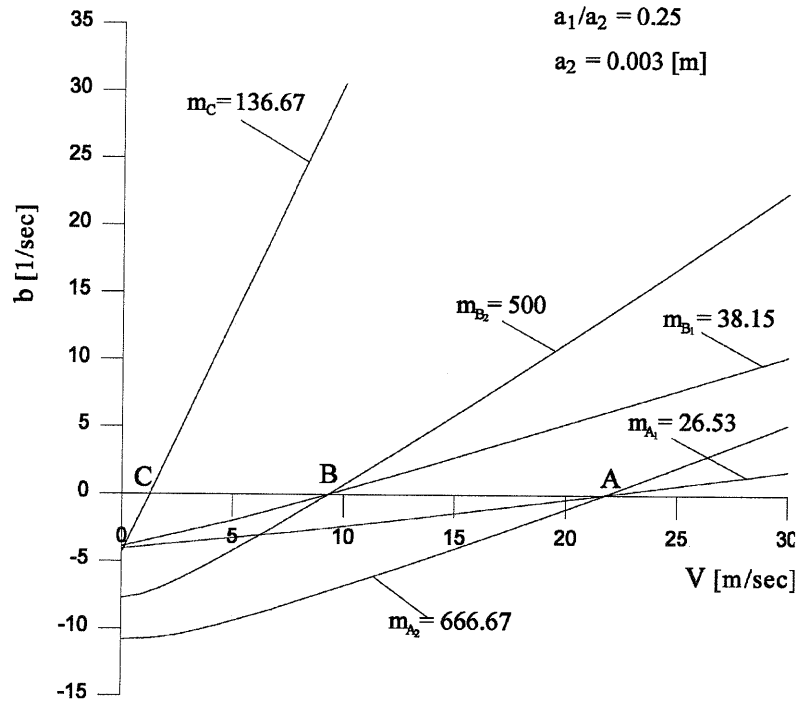


Fig. 3. Variation of the growth rate  $b$  against the sliding speed  $V$  for different values of the wave number  $m$  ( $a_1/a_2 = 0.25$  and  $a_2 = 0.003$  (m)).

each sliding speed. This in fact permits to define the function  $b(t) = b(V(t))$ , as described in Section 3.2. Tacitly, it is assumed here that contact is maintained at all times along the sliding interface.

In Fig. 3, the curves  $b(V)$  are shown for three working conditions listed above, and a typical value of  $a_2 = 3$  (mm). The perturbation with the lowest critical speed (point C) is also associated with the highest growth rate, thus it is the absolutely dominant perturbation. In addition, comparing perturbations with identical sliding speeds but different wave numbers (points  $A_1 - A_2$  and  $B_1 - B_2$ ), it can be deduced that the smaller the wave number the lower the growth rate. Therefore, perturbations with lower wave numbers are less critical. However, it must be noticed that the finite circular extension of disks in clutches and brakes imposes a limit on the minimum supportable wave number, or maximum wave length, as observed in Lee and Barber [5]. If a mean radius  $R_m$  of the disk is considered, the wave length  $\lambda = 2\pi/m$  of the perturbation has to be a submultiple of the medium circumferential length  $2\pi R_m$ , that is

$$\lambda = \frac{2\pi R_m}{N} \quad \text{or conversely} \quad m = \frac{N}{R_m} \quad (16)$$

where  $N$  is the number of hot spots. In Table 2, for  $R_m = 50$  (mm), the wave length and the wave number corresponding to different values of  $N$  are listed. Clearly, perturbation with  $m < 20$  ( $\text{mm}^{-1}$ ) must not be considered.

Fig. 4, presents the variation of the dimensionless growth rate  $\tilde{b}(= b/m^2 k_2)$  with the dimensionless sliding speed

$\tilde{V}(= Va_2/k_2)$  for a fixed wave parameter ( $ma_2 = 1.5$ ) and different values of the thickness ratio, namely  $a_1/a_2 = 0.2, 0.25, 0.3$ . It is observed that as the ratio  $a_1/a_2$  increases, the growth rate decreases at fixed sliding speed, whilst the critical speed increases. Therefore, the effect of increasing the thickness ratio is that of reducing the susceptibility towards hot spotting (critical speed increase) and the severity of the thermomechanical damage (growth rate decrease). Notice that such a result obliges to rethink at the classical clutches and brakes design procedures where thicker metal disks are preferred to reduce the mean temperature of the system and thinner friction layers are employed to reduce costs and duration of the engagement cycle: what is beneficial for classical design is deleterious for TEI.

In addition, the effect of the material properties on the growth rate,  $b$  is shown in Fig. 5, as a function of the sliding speed. Two sets of materials are considered as from Table 1: a brake friction material which is less compliant and more conductive than a clutch friction material. Friction materials

Table 2  
Wave length and wave number for different values of  $N$  ( $R_m = 50$  (mm))

$\lambda$ (mm)	$m$	$N$
314	20	1
157	40	2
78.5	80	4
39.25	160	8
19.625	320	16

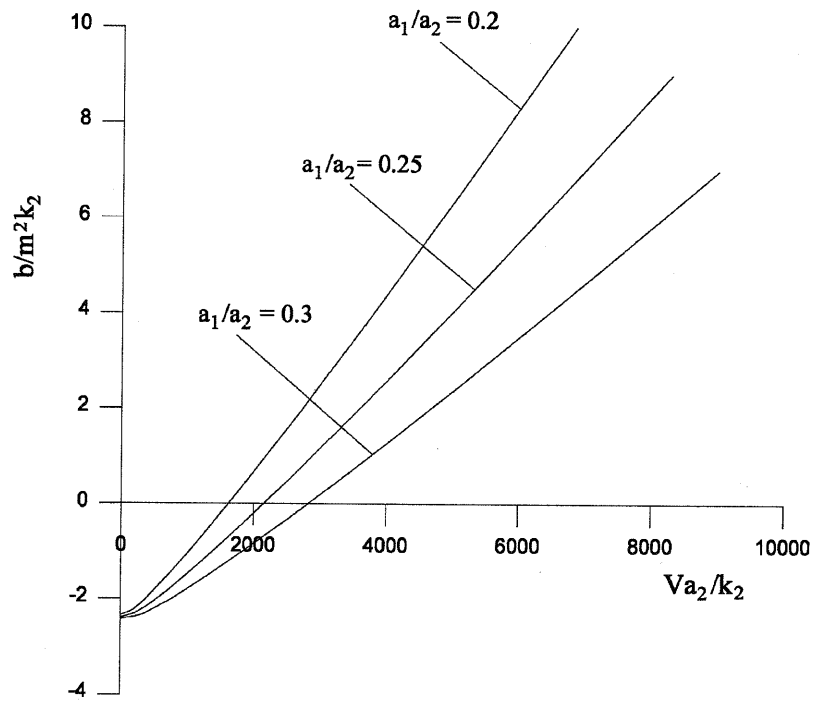


Fig. 4. Variation of the dimensionless growth rate  $\tilde{b} = b/m^2k_2$  against the sliding speed  $\tilde{V} = Va_2/k_2$ , for different values of the thickness ratio  $a_1/a_2$  ( $ma_2 = 1.5$ ).

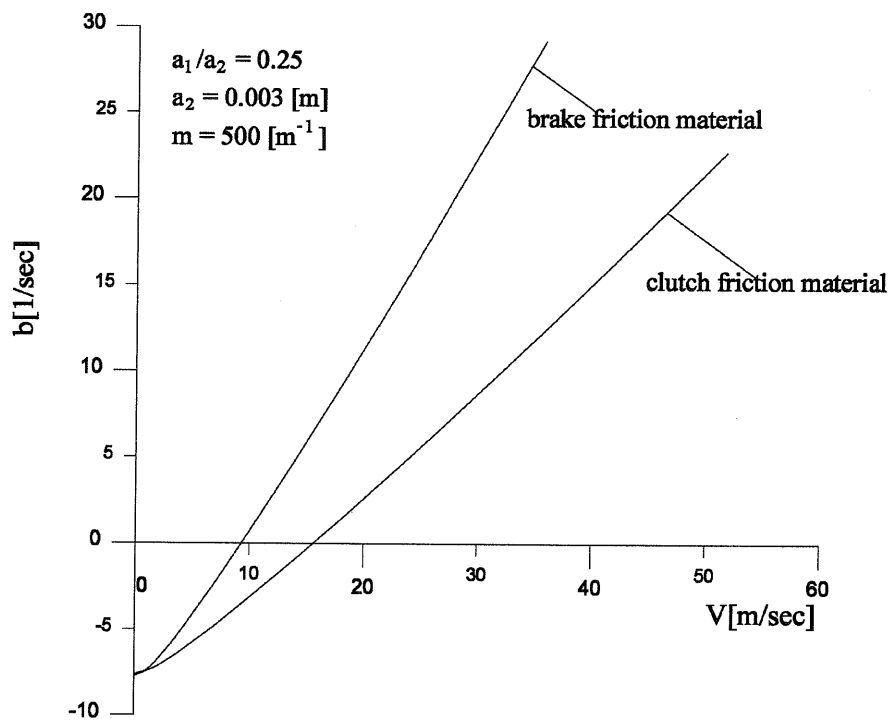


Fig. 5. Variation of the growth rate  $b$  against the sliding speed  $V$  for two different sets of friction materials.

used in clutches are less prone to thermoelastic instability leading to a larger critical speed and smaller growth rates. On the contrary, brake friction materials with larger elastic modulus, i.e. smaller wear rates, are generally more susceptible to TEI.

### 3.2. Transient evolution of the temperature field

Al-Shabibi and Barber [12] have shown that surface pressure and temperature in the transient regime can be written as

$$T = T(0) \exp \left\{ \int_0^t b(V(t)) dt \right\} \quad (17)$$

$$p = p(0) \exp \left\{ \int_0^t b(V(t)) dt \right\} \quad (18)$$

where  $T(0)$  and  $p(0)$  are the temperature and contact pressure at the time  $t = 0$ , and  $b(t)$  is the dominant growth rate at each speed  $V(t)$ . The above two expressions derive from the fact that the transient evolution of the system with  $V(t)$  can be considered as the superposition of quasi-static problems with different sliding speeds, corresponding at different time instants. In that case the temperature field is given by an eigenfunction series as  $T(x, y, t) = \sum_{i=1}^n C_i e^{b_i t} \theta_i(x, y)$ , where  $C_i$  is an arbitrary constants determined from the initial condition  $T(x, y, z, 0)$ . However, the transient response

is dominated by the term with the largest value of  $b_i$ , which is the only that needs to be considered. Thus,

$$\begin{aligned} T(x, y, t) &= C_i e^{b_i t} \theta_i(x, y) \rightarrow \frac{\partial T}{\partial t} \\ &= C_{\text{dom}} b_{\text{dom}} e^{b_{\text{dom}} t} \theta_{\text{dom}}(x, y) = b_{\text{dom}} T(x, y) \end{aligned} \quad (19)$$

where  $b_{\text{dom}}$  is the dominant growth rate at a fixed sliding speed.

Therefore, knowing the variation of  $b$  with  $V$  from the characteristic equation for fixed geometry and material parameters, and assuming that during a clutch/brake engagement process the sliding speed  $V$  reduces linearly with time  $V(t) = V_0(1 - t/t_0)$ , from Eqs. (17) and (18), the transient evolution of the temperature and pressure at the sliding interface can be derived.

The evolution with time of the temperature amplitude normalized with respect to its initial value  $T(0)$  is shown in Fig. 6, for fixed layers' thickness. In agreement with what depicted in Fig. 3, perturbations with lower wave number leads to lower temperature increase (points A and B). Therefore, for fixed sliding speeds, perturbations with larger wave numbers cause more intense thermomechanical damages.

In Figs. 7 and 8, the evolution of the normalized temperature  $T/T(0)$  with respect to the dimensionless time  $\tau = k_2 m^2 t$  is presented, for wave number higher and lower than

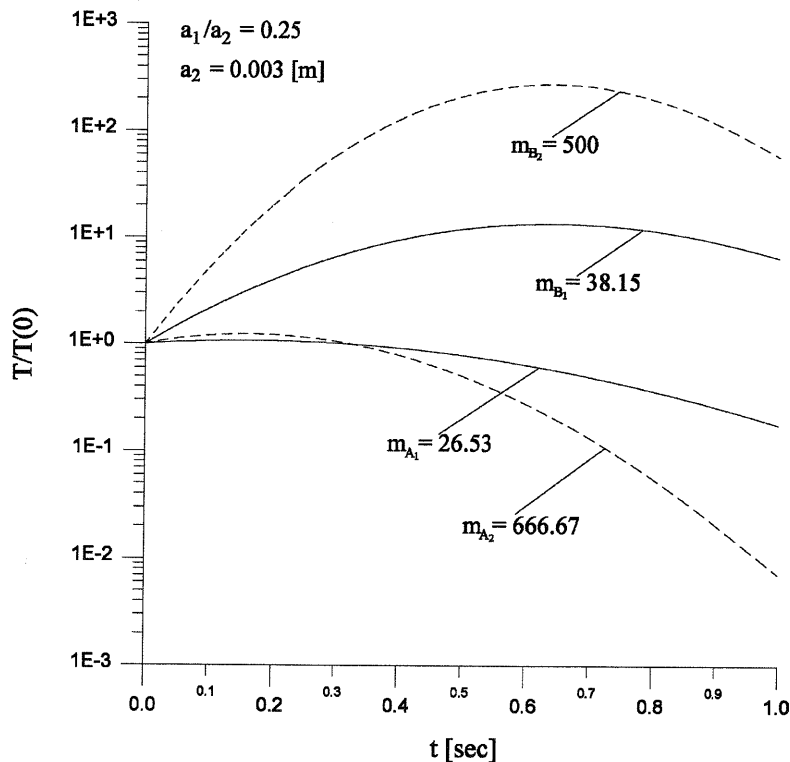


Fig. 6. Transient evolution of the normalized temperature  $T/T(0)$  for sliding speed decreasing linearly with time.

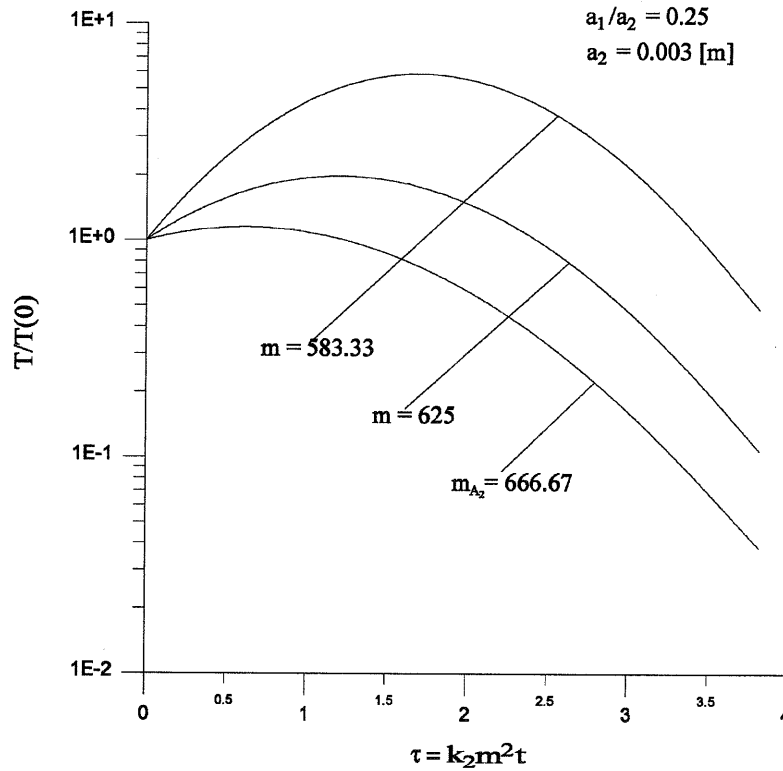


Fig. 7. Transient evolution of the normalized temperature  $T/T(0)$  for sliding speed decreasing linearly with time: wave numbers greater than the critical value ( $m_{cr} = 136.67 \text{ (m}^{-1}\text{)}$ ).

the critical value  $m_{cr} = m_C = 136.67 \text{ (m}^{-1}\text{)}$ . Two different trends are found:

- the temperature increases with  $m$  (Fig. 7), for perturbations with  $m < m_{cr}$ ;
- the temperature decreases with  $m$  (Fig. 8), for perturbations with  $m > m_{cr}$ .

From Fig. 9, where the transient evolution of the normalized temperature  $T/T(0)$  is shown for different thickness ratio ( $a_1/a_2 = 0.275; 0.2925; 0.3$ ) and  $ma_2 = 1.5$ , it can be derived that a small reduction of  $a_1/a_2$  leads to a large increase of the temperature.

### 3.3. Approximated analysis of the transient temperature field

From Fig. 3, it can be observed a fairly linear variation of the growth rate with the sliding speed. Thus, an approximate expression for  $\tilde{b} = \tilde{b}(\tilde{V})$  can be written as

$$\tilde{b}^* = \eta \tilde{V} + \xi \quad (20)$$

where the coefficient  $\eta$  and  $\xi$  depends on the thickness ratio and wave parameter. Once  $a_1/a_2$  and  $ma_2$  have been fixed,  $\eta$  and  $\xi$  can be calculated with a classical least squares method. In particular for  $ma_2 = 1.5$ , the values of  $\eta$  and  $\xi$  are listed in Table 3 for different thickness ratio.

It is tempting to think that a simple relationship between the parameters  $\eta$  and  $\xi$  and the wave parameter  $ma_2$  could exist. Unfortunately, it has been verified that this is not the case, thus  $\eta$  and  $\xi$  should be determined for each  $ma_2$  independently.

A comparison between the actual solution (dashed line) and the approximate solution (solid line) is presented in Fig. 10, using the values given in Table 3. The largest deviations are observed for negative growth rates as the sliding speed goes to zero, which are not of practical interest (decaying perturbations). Also, the error on the critical speed ( $b = 0$ ) is generally smaller than 5%. Consequently, the linear approximation proposed can be employed to estimate the evolution of the system, and considering again a linearly decreasing sliding speed, from (17) an explicit formula is obtained for the transient evolution of the temperature

$$T = T(0) \exp \left\{ (\eta \tilde{V}_0 + \xi) \tau - \frac{\eta \tilde{V}_0}{2\tau_0} \tau^2 \right\} \quad (21)$$

Table 3  
Coefficients for the linear relation  $\tilde{b}(\tilde{V})$

$a_1/a_2$	$\eta$	$\xi$
0.25	$1.37 \times 10^{-3}$	-2.865
0.275	$1.19 \times 10^{-3}$	-2.828
0.3	$1.02 \times 10^{-3}$	-2.782

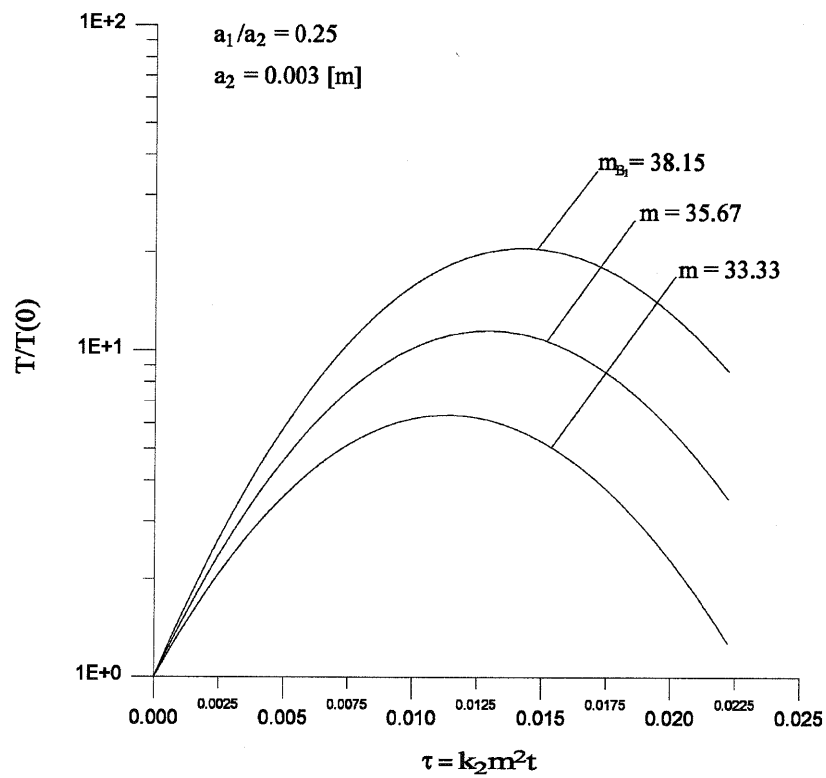


Fig. 8. Transient evolution of the normalized temperature  $T/T(0)$  for sliding speed decreasing linearly with time: wave numbers smaller than the critical value ( $m_{cr} = 136.67$  ( $m^{-1}$ )).

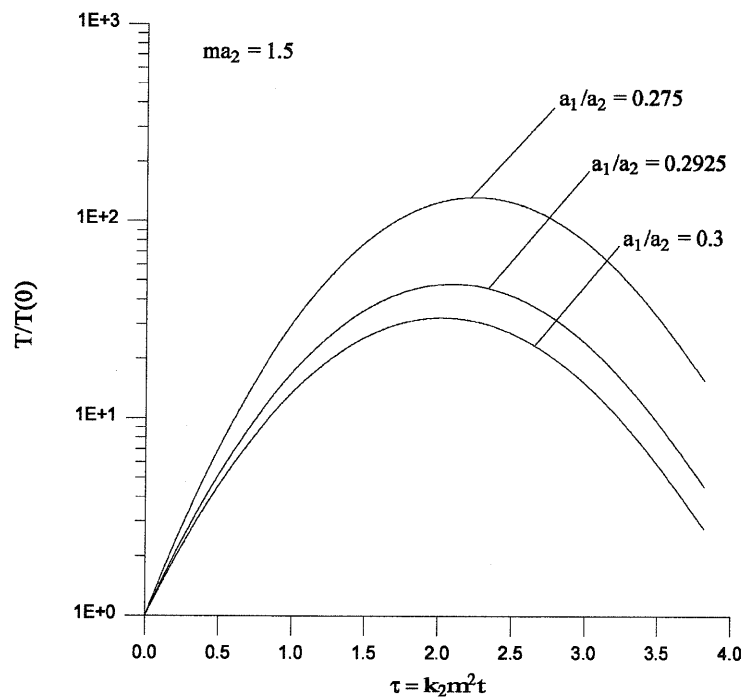


Fig. 9. Transient evolution of the normalized temperature  $T/T(0)$  for sliding speed decreasing linearly with time, for different values of the thickness ratio  $a_1/a_2$  ( $ma_2 = 1.5$ ).

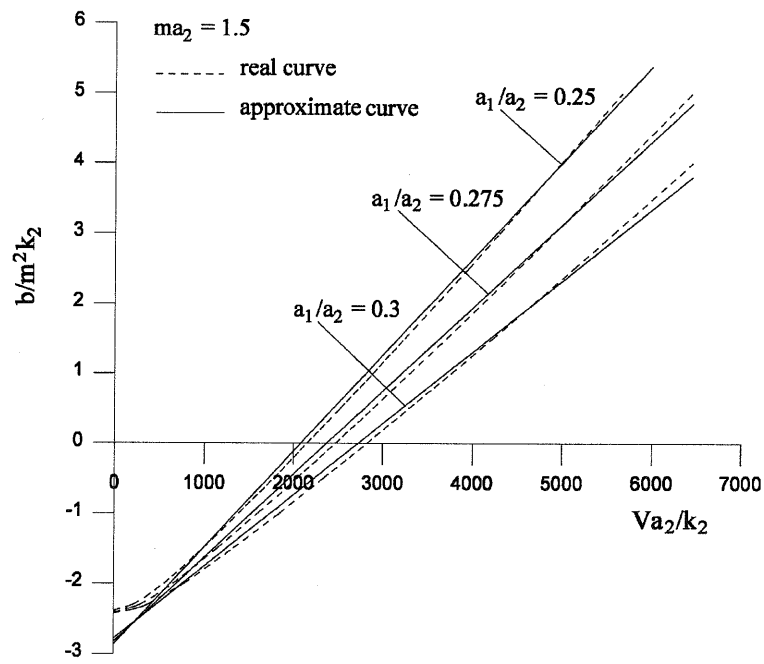


Fig. 10. Growth rate-sliding speed curves: a comparison between the approximate (solid line) and actual solution (dashed line).

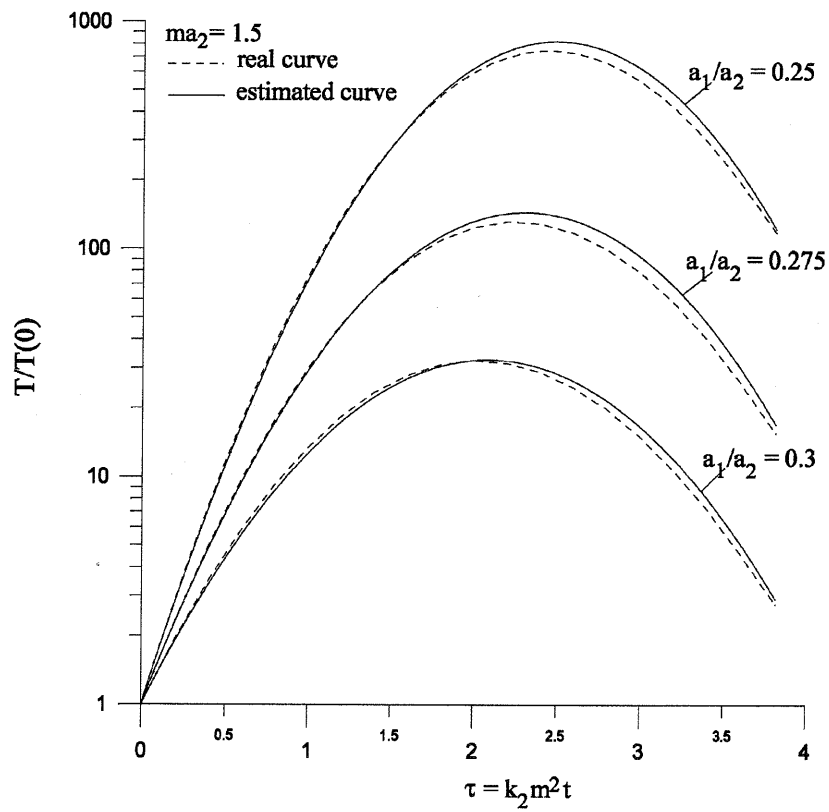


Fig. 11. Normalized temperature-time curves: a comparison between the approximate (solid line) and actual solution (dashed line).

In Fig. 11 (Eq. (21)) (solid line) is compared with the actual solution (dashed line), for  $\tilde{V}_0 = 6000$  and  $\tau_0 = 3.82$ . The approximated curves overestimate slightly the temperature growth, and the percentage difference is generally smaller than 10%.

It is possible indeed to approximate the curve  $b(V)$  linearizing the sole positive part of the curve, i.e.  $V > V_{cr}$ . However the improvement with respect to the above proposed linearization is generally negligible.

#### 4. Conclusions

A small perturbation analysis of a 2D multilayered model has been performed beyond the onset of instability for TEI ( $b > 0$ ). The model reproduces the finite thickness of the disks and the actual material properties used in clutches and brakes for automotive applications.

The variation of the growth rate  $b$  with the operative sliding speed  $V$  has been studied and it has been found that (i) the perturbation with the lowest critical speed has also the highest growth rate, i.e. it is the absolutely dominant perturbation; (ii) when comparing perturbations with identical critical speed, those with smaller wave numbers have lower growth rates and are then less critical. In addition, it is observed that the growth rate  $b$  decreases at fixed sliding speed as the thickness ratio  $a_1/a_2$  increases, thus confirming that thinner metal disks and thicker frictional disks not only reduce the susceptibility towards hot spotting (critical speed increase) but they also reduce the severity of thermomechanical damage (growth rate decrease).

From the analysis of the transient evolution of the temperature field, it has been derived that (i) when comparing perturbations with identical critical speed, those with higher wave numbers cause more intense thermomechanical damages (larger growth rate); (ii) for perturbations with  $m < m_{cr}$  (critical wave number) the temperature increases with  $m$ ; whilst for perturbations with  $m > m_{cr}$  the temperature decreases with  $m$ ; (iii) the surface temperature increases as  $a_1/a_2$  reduces.

Finally, it has been observed that in general the relation  $b(V)$ , between the growth rate and the sliding speed, for a given perturbation can be approximated by a linear regression. Consequently, assuming an engaging speed linearly decreasing with time, a closed form solution for the evolution of the temperature distribution with time has been proposed

as a function of the engagement conditions. For geometry and material properties typical of automotive applications, the difference between the approximated and actual solution is smaller than 10%.

#### Acknowledgements

The authors wish to thank Prof. James R. Barber of the University of Michigan for his helpful comments and to acknowledge the Center of Excellence in Computational Mechanics at the Politecnico di Bari for financial support. Paolo Decuzzi wish to thank Raybestos Products Company for supporting his stay at the University of Michigan and at RayTech.

#### References

- [1] P. Decuzzi, M. Ciavarella, G. Monno, Frictionally excited thermoelastic multi-disk clutches and brakes, *ASME J. Tribol.* 123 (2001) 865–871.
- [2] R.C. Parker, P.R. Marshall, The measurement of temperature of sliding surfaces with particular reference to railway blocks, *Proc. Inst. Mech. Engrs.*, London 158 (1948) 209–229.
- [3] J.R. Barber, Thermoelastic instabilities in the sliding of conforming solids, *Proc. Roy. Soc., London, Ser. A* 312 (1969) 381–394.
- [4] R.A. Burton, V. Nerlikar, S.R. Kilaparti, Thermoelastic instability in a seal-like configuration, *Wear* 24 (1973) 189–198.
- [5] K. Lee, J.R. Barber, Frictionally-excited thermoelastic instability in automotive disk brakes, *ASME J. Tribol.* 115 (1993) 607–614.
- [6] K. Lee, J.R. Barber, The effect of shear traction on frictionally-excited thermoelastic instability, *Wear* 160 (1993) 237–242.
- [7] Y.-B. Yi, J.R. Barber, P. Zagrodzki, Eigenvalue solution of thermoelastic instability problems using Fourier reduction, *Proc. Roy. Soc., London, Ser. A* 456 (2000) 2799–2821.
- [8] P. Decuzzi, G. Demelio, The effect of material properties on the thermoelastic stability of sliding systems, *Wear* 252 (2002) 311–321.
- [9] C.L. Davis, C.M. Krousgrill, F. Sadeghi, Effect of temperature on thermoelastic instability in thin disks, *J. Tribol.* 124 (2002) 429–437.
- [10] P. Zagrodzki, Analysis of thermomechanical phenomena in multi-disk clutches and brakes, *Wear* 140 (1990) 291–308.
- [11] J.Y. Jang, M.M. Khonsari, Thermal characteristics of a wet clutch, *J. Tribol.* 121 (3) (1999) 610–617.
- [12] A.M. Al-Shabibi, J.R. Barber, Transient solution of a two-dimensional TEI problem using a reduced order model, *Int. J. Mech. Sci.* 44 (2002) 451–464.
- [13] J.R. Barber, *Elasticity*, Kluwer Academic Publishers, Boston, 1992.
- [14] A.E. Green, W. Zerna, *Theoretical Elasticity*, Clarendon Press, Cambridge, 1954.